AEDC-TR-75-122

Cy.2

STATIC STABILITY AND AXIAL FORCE TESTS OF THE HOLLOMAN MONORAIL ROCKET SLED AT MACH NUMBERS 8 AND 10

VON KÁRMÁN GAS DYNAMICS FACILITY
ARNOLD ENGINEERING DEVELOPMENT CENTER
AIR FORCE SYSTEMS COMMAND
ARNOLD AIR FORCE STATION, TENNESSEE 37389

February 1976

Final Report for Period January 15 – May 9, 1975

Prepared for

AIR FORCE SPECIAL WEAPONS CENTER
6585TH TEST GROUP (TKE)
HOLLOMAN AIR FORCE BASE, NEW MEXICO 88330

NOTICES

When U. S. Government drawings specifications, or other data are used for any purpose other than a definitely related Government procurement operation, the Government thereby incurs no responsibility nor any obligation whatsoever, and the fact that the Government may have formulated, furnished, or in any way supplied the said drawings, specifications, or other data, is not to be regarded by implication or otherwise, or in any manner licensing the holder or any other person or corporation, or conveying any rights or permission to manufacture, use, or sell any patented invention that may in any way be related thereto.

Qualified users may obtain copies of this report from the Defense Documentation Center.

References to named commercial products in this report are not to be considered in any sense as an endorsement of the product by the United States Air Force or the Government.

This report has been reviewed by the Information Office (OI) and is releasable to the National Technical Information Service (NTIS). At NTIS, it will be available to the general public, including foreign nations.

APPROVAL STATEMENT

This technical report has been reviewed and is approved for publication.

FOR THE COMMANDER

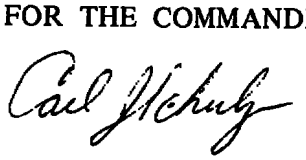

CARL J. SCHULZE
Major, USAF
Chief Air Force Test Director, VKF
Directorate of Test

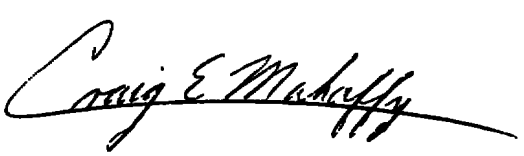

CRAIG E. MAHAFFY
Colonel, USAF
Director of Test

REPORT DOCUMENTATION PAGE	READ INSTRUCTIONS BEFORE COMPLETING FORM
1 REPORT NUMBER: AEDC-TR-75-122	2. GOVT ACCESSION NO. / 3 RECIPIENT'S CATALOG NUMBER
4 TITLE (and Subtitle): STATIC STABILITY AND AXIAL FORCE TESTS OF THE HOLLOMAN MONORAIL ROCKET SLED AT MACH NUMBERS 8 AND 10	5 TYPE OF REPORT & PERIOD COVERED: Final Report - January 15 - May 9, 1975
	6 PERFORMING ORG. REPORT NUMBER
7. AUTHOR(s): R. W. Rhudy and J. D. Corce - ARO, Inc.	8. CONTRACT OR GRANT NUMBER(s)
9 PERFORMING ORGANIZATION NAME AND ADDRESS: Arnold Engineering Development Center (XO), Arnold Air Force Station, Tennessee 37389	10 PROGRAM ELEMENT, PROJECT, TASK AREA & WORK UNIT NUMBERS: Program Element 65807F, System 921A
11. CONTROLLING OFFICE NAME AND ADDRESS: Air Force Special Weapons Center, 6585th Test Group (TKE), Holloman Air Force Base, NM 88330	12 REPORT DATE: February 1976
	13. NUMBER OF PAGES: 29
14 MONITORING AGENCY NAME & ADDRESS(if different from Controlling Office)	15. SECURITY CLASS. (of this report): UNCLASSIFIED
	15a. DECLASSIFICATION/DOWNGRADING SCHEDULE: N/A

16. DISTRIBUTION STATEMENT (of this Report)

Approved for public release; distribution unlimited.

17 DISTRIBUTION STATEMENT (of the abstract entered in Block 20, if different from Report)

18 SUPPLEMENTARY NOTES

Available in DDC

19 KEY WORDS (Continue on reverse side if necessary and identify by block number)

static stability
rocket sled
hypersonic flow
Reynolds number
aerodynamic characteristics

20 ABSTRACT (Continue on reverse side if necessary and identify by block number)

Experimental static-stability and axial-force data are presented for several configurations of a 0.4-scale model of a Monorail Rocket Sled at Mach numbers of 8 and 10. The test Reynolds numbers, based on maximum model length, were approximately 14.4 and 10.7 million, respectively. The models were tested in close proximity to a ground plane assembly which simulated the rail and trough of the Holloman AFB High-Speed Test Track. Results are presented to show the effects of configuration variables such as nose shape; vertical,

DD FORM 1 JAN 73 1473 EDITION OF 1 NOV 65 IS OBSOLETE

20. ABSTRACT (Continued)

forward, and aft canards; rocket booster chamber length; and forward and aft slipper wedges.

AFSC
Arnold AFS Tenn

PREFACE

The work reported herein was conducted by the Arnold Engineering Development Center (AEDC), Air Force Systems Command (AFSC), at the request of the Air Force Special Weapons Center (AFSWC), under Program Element 65807F, System 921A. The monitor for this project was Mr. D. J. Krupovage, 6585th Test Group/TKE, Holloman AFB, New Mexico. The results were obtained by ARO, Inc. (a subsidiary of Sverdrup & Parcel and Associates. Inc.), contract operator of AEDC, AFSC, Arnold Air Force Station, Tennessee. The work was done under ARO Project No. V41A/B-45A. The authors of this report were R. W. Rhudy and J. D. Corce, ARO, Inc. Data reduction was completed on June 6, 1975, and the manuscript (ARO Control No. ARO-VKF-TR-75-122) was submitted for publication on July 23. 1975.

CONTENTS

ILLUSTRATIONS

TABLES

1.0 INTRODUCTION

The purpose of this investigation was to determine the static stability and axial-force characteristics of the Monorail Rocket Sled in the presence of a track and ground plane. As pointed out in Ref. 1, the sled bow wave interaction with the boundary layer on the ground plane and rail surfaces differs from the actual case; however, previous investigations have shown reasonable correlations between wind tunnel data and actual track tests. The current data were obtained on several sled configurations in the 50-in. Hypersonic Wind Tunnels (B) and (C) of the von Kármán Gas Dynamics Facility (VKF) at Mach numbers of 8 and 10 at free-stream unit Reynolds numbers of approximately 3.5 and 2.6 million per ft, respectively. The configuration variables were nose shape; vertical, forward, and aft canards; rocket booster chamber length; and forward and aft slipper wedges. In addition to the force and moment data, base pressures and flow-field shadowgraph photographs were obtained at all test conditions at the nominal test angle of attack of zero degree.

2.0 APPARATUS

2.1 WIND TUNNEL

Tunnels B and C are closed-circuit, hypersonic wind tunnels with 50-in.-diam test sections. Axisymmetric contoured nozzles are available to provide Mach numbers of 6 and 8 in Tunnel B and 10 in Tunnel C. The tunnels may be operated continuously over a range of pressure levels from 20 to 300 psia at $M_\infty = 6$, 50 to 900 psia at $M_\infty = 8$, and 200 to 2,000 psia at $M_\infty = 10$, with air being supplied by the VKF main compressor plant. Tunnel B stagnation temperatures sufficient to avoid air liquefaction in the test section (up to 1,350°R) are obtained through the use of a natural gas fired combustion heater, while Tunnel C temperatures (up to 1,900°R) are obtained through the use of the gas fired heater in series with an electric resistance heater. The tunnels (throats, nozzles, test sections, and diffusers) are cooled with external water jackets. Model injection systems are employed which allow the removal of a model from the test section while the tunnel remains in operation.

2.2 MODEL

The 0.4-scale Monorail Rocket Sled model and ground plane assembly, designed and fabricated by Systems Research Laboratories, is shown installed in Tunnel B in Fig. 1 and schematically in Figs. 2 and 3. The four nose shapes tested were an 18-deg standard nose cone, a 22-deg shock ingestion nose shape, a biconic shock ingestion nose, and a one-half cone 6-deg shock ingestion nose (see Fig. 4). Two sizes of forward canards were

tested, the smaller being cut from the originals. Figure 5 shows the details of the forward and aft slipper canards (both tested at a 25-deg deflection). The upper and lower vertical canards (see Fig. 6) were always tested at zero deflection. The forward and aft slipper wedges, tested on and off, are shown in Fig. 7. The slipper support details are shown in Fig. 8. The forward canards, vertical canards, and forward and aft wedges were tested only with the 18-deg standard nose cone shape, while the aft canards were tested with all four noses.

The overall length of the sled model was a variable because it was apparent that a wake interference problem would be caused by the close proximity of the sting flare and other equipment to the base of the model (see Fig. 2). Therefore, most configurations were run with a 6-in. piece of the booster chamber removed (see Fig. 3). It should be noted that, with the 6-in. piece removed, the model configuration was no longer an exact simulation of the full-scale sled.

The model, supported by a balance and sting, could be manually adjusted in pitch and height by yokes attached to the sting to obtain clearance between the slippers and the rail (see Fig. 2). Fouling lights and television cameras were used to indicate when contact existed between the model slippers and the rail. The design rail-to-slipper clearance dimensions are shown in Fig. 9. Carborundum® grit was used on the model nose to promote a turbulent boundary layer.

2.3 INSTRUMENTATION

Tunnel B stilling chamber pressure is measured with a 100- or 1,000-psid transducer referenced to a near vacuum. Based on periodic comparisons with secondary standards, the uncertainty (a bandwidth which includes 95 percent of residuals) of the transducers is estimated to be within ±0.1 percent of reading or ±0.06 psi, whichever is greater, for the 100-psid range and ±0.1 percent of reading or ±0.5 psi, whichever is greater, for the 1,000-psid range. Tunnel C stilling chamber pressure is measured with a 500- or 2,500-psid transducer referenced to a near vacuum. The uncertainty of the transducers is estimated to be within ±0.1 percent of reading or ±0.25 psi whichever is greater for the 500-psid range and ±0.1 percent or reading or ±1.25 psi whichever is greater for the 2,500-psid range. Stilling chamber temperature measurements are made with Chromel®-Alumel® thermocouples which have an uncertainty of ±(1.5°F + 0.375 percent of reading) based on repeat calibrations.

Model forces and moments were measured with a six-component, moment-type, strain-gage balance supplied and calibrated by VKF. Prior to the test, static loads in each plane and combined static loads were applied to the balance to simulate the range of

loads and center-of-pressure locations anticipated during the test. The following uncertainties represent the bands of 95 percent of the measured residuals, based on differences between the applied loads and the corresponding values calculated from the balance calibration equations included in the final data reduction.

UNCERTAINTY IN VKF -050 BALANCE

Component	Balance Design Loads	Range of Static Loads	Measurement Uncertainty
Normal force, lb	±200	±40.0	±0.25
Pitching moment, in.-lb*	±680	±19.0	±0.90
Side force, lb	±200	± 1.5	±0.20
Yawing moment, in.-lb*	±680	± 3.0	±0.70
Rolling moment, in.-lb	±100	± 4.0	±0.15
Axial force, lb	50	0 to 20.0	±0.12

*About balance forward moment bridge.

The transfer distances from the balance forward moment bridge to the model moment reference location were 17.74 and 23.74 in. along the longitudinal axis and 0 in. along the vertical axis and were measured with an estimated precision of ±0.01 in.

The base pressures were measured with 15-psid transducers referenced to a near vacuum and having full-scale calibration ranges of 1, 5, and 15 psia. Based on periodic comparison with secondary standards, the precision of these transducers are estimated to be ±0.2 percent of reading or ±0.01 psi, whichever is greater.

Model flow-field shadowgraphs were obtained on all configurations to show the extent of shock interaction between the sled, rails, and ground plane.

3.0 PROCEDURE

3.1 TEST CONDITIONS

The investigation was conducted at Mach numbers of 8 and 10 at the maximum possible Reynolds numbers. A summary of the nominal test conditions is given below:

M_∞	8.0	10.0
p_o, psia	800	2,000
T_o, °R	1,330	1,890
p_∞, psia	0.082	0.046
q_∞, psia	3.67	3.25
$Re_{\infty,d} \times 10^6$	0.73	0.54

3.2 TEST PROCEDURE

Prior to injection into the tunnel test section, a nominally uniform alignment of the sled slippers along the rail in pitch was accomplished by use of the pitch-height yokes attached to the ground plane. The alignment of the slippers in yaw with respect to the rail was also adjusted to provide nearly uniform clearance between the slippers and the sides of the rail. Zero pitch and roll were set on the ground plane to within ±0.1 deg by use of an inclinometer. The slipper clearances were monitored during all data acquisition by use of "foul" lights and four closed-circuit television cameras focused on both sides of the two slippers.

The actual test runs were conducted in a rapid manner since the high temperature of the flow in Tunnels B and C could cause the sled model, rail, and ground plane to warp within several seconds of injection. Once injected, the slippers would occasionally "foul out" on the rail due to aerodynamic loading, whereupon the sled was retracted and the pitch of the model with respect to the rail varied in an attempt to anticipate the air load deflections. The data sequence was then repeated. When a model setting was found which did not foul in the tunnel, data were taken until thermal warpage of the model and rail assembly caused contact to occur. Each data point consisted of an average of 50 samples of each component taken at a rate of 78 samples per second.

Two sled base pressures were measured adjacent to the sting in the horizontal plane and used to correct the total axial force at all test conditions. Model flow-field shadowgraphs were obtained on all configurations to show the extent of shock interaction between the sled, rail, and ground plane.

3.3 DATA PRECISION

An evaluation of the influence of random-measurement errors is given in this section to provide a partial evaluation of the precision of the data presented. No evaluation of the systematic measurement error (bias) is included. Uncertainties (bands which include 95 percent of the calibration data) in the basic tunnel parameters (p_o, T_o, and M_∞) were

estimated from repeat calibrations of the instrumentation (see Section 2.3) and from the repeatability and uniformity of the test section flow during tunnel calibrations. These uncertainties were then used to estimate uncertainties in the other free-stream properties for the primary test conditions.

M_∞	8.0	10.0
M_∞	±0.02	±0.05
p_o, psia	±0.80	±2.00
T_o, °R	±5.3	±7.5
p_∞, psia	±0.0013	±0.0016
q_∞, psia	±0.0407	±0.0759

The aerodynamic coefficient uncertainties listed below were obtained using the maximum and minimum values of the entire test regardless of configurations. The balance uncertainties listed in Section 2.3 are combined with the uncertainties in the tunnel parameters using the Taylor series method of error propagation, to estimate the precision of the coefficients.

	M_∞ = 8.0		M_∞ = 10.0	
	Relative Uncertainty, near Max Value (± percent)	Absolute Uncertainty, near min Value (±)	Relative Uncertainty, near Max Value (± percent)	Absolute Uncertainty, near Min Value (±)
C_N	2.48	0.009	4.07	0.010
C_m	2.31	0.087	3.81	0.097
C_{A_t}	1.30	0.004	2.46	0.005
C_A	1.33	0.006	2.51	0.008

Based on the maximum possible variation in forward and aft slipper clearance with respect to the rail, the sled was aligned in pitch with respect to the rail within ±0.2 deg for the longest sled configuration (booster chamber length 27.09 in.) and within ±0.4 deg for the shortest sled configuration (booster chamber length 19.59 in.). Since the rail and ground plane were aligned with respect to the tunnel flow within ±0.1 deg, a few configurations may have had a maximum angle of attack of ±0.5 deg. The variation in the slipper clearances is thought to have little effect on the values of the aerodynamic coefficients. This is based on results presented in Ref. 2 for a four-slipper, Narrow-Gage Rocket Sled that was tested with the slipper clearances being a test variable. The Narrow-Gage Sled was approximately 20 in. in length, had a body diameter of 3.0 in., and rode on two rails with a slipper-rail clearance greater than full scale that produced only second-order effects.

4.0 RESULTS AND DISCUSSION

A complete tabulation of the results from this investigation is given in Table 1. These data are an average of several points that were taken on one or more injections into the tunnel and, in most cases, in the absence of slipper contact with the rail. Configurations where contact may have occurred are noted in the table.

Figure 10 shows typical shadowgraphs of the number 1 and 3 noses at $M_\infty = 8$. This photograph shows that there was some interference between the rail leading-edge shock and the number 1 bow wave. The photograph also shows the ingestion of the reflected bow wave from the number 3 nose.

As pointed out earlier, interference between the sting and the model base dictated the shortening of the booster for the majority of the testing. This shorter configuration was, therefore, not to scale in length; however, enough data were obtained on the longer configuration to determine that the effect of booster length on the aerodynamic coefficients was minimal. Even with the shorter configuration, there probably was base and/or wake interference since in most cases forebody axial-force coefficient (C_A) was higher than total axial-force coefficient (C_{A_t}).

Typical configuration buildup data for the number 1 nose are shown graphically in Fig. 11. These data along with the tabulated data show that in most cases, the normal force coefficient (C_N) resulting from the various model components in conjunction with the number 1 nose shape was from 30 to 80 percent higher at Mach number 10 than at Mach number 8. This higher normal force resulted in larger (more negative) pitching-moment coefficients (C_m) about the aft slipper. The Mach number 10 C_A was, however, slightly lower (approximately 5 to 10 percent) than the Mach number 8 data.

During the Mach number 8 testing, it was determined that the original design of the forward canards produced a restoring moment, about the aft slipper, far greater than anticipated. These canards were reduced in size (see Fig. 5) by cutting off the trailing edge. The canard area reduction (25 percent) resulted in a 20- to 50-percent reduction in C_m, depending on the other configuration variables. The large canards were not tested at $M_\infty = 10$.

For the other nose shapes (2, 3, and 4), all of the aerodynamic coefficients were lower at $M_\infty = 10$ than at $M_\infty = 8$. The reduction in C_A, as Mach number was increased, was about 10 to 15 percent.

The wind tunnel aerodynamic coefficients were converted to the full-scale sled loads presented in Table 2 using a static pressure of 12.7 psia which corresponds to a pressure

altitude of 4,000 ft. Because of the large increase in dynamic pressure as Mach number was increased from 8 to 10 at constant altitude, the slipper normal loads and moments for all configurations were, at times, more than twice as high at M_∞ = 10 than at M_∞ = 8. While the forebody axial-force coefficient was reduced with an increase in Mach number, the full-scale loads were increased by as much as 50 percent when the Mach number was increased from 8 to 10.

5.0 CONCLUDING REMARKS

Static force and moment tests were conducted on several configurations of the Monorail Rocket Sled at Mach numbers of 8.0 and 10.0. Based on the results presented, the following observations are noted:

1. A general increase in C_N and C_m occurred when Mach number was increased from 8 to 10 on the number 1 nose configuration.

2. The number 2 through 4 nose configurations produced a decrease in C_N and C_m with an increase in M_∞.

3. The forebody axial-force coefficient was lower for all configurations at M_∞ = 10 than at M_∞ = 8.

4. Because of the nearly 60-percent increase in dynamic pressure, all of the full-scale loads at M_∞ = 10 were much higher than at M_∞ = 8.

REFERENCES

1. Strike, W. T. and Lucas, E. J. "Evaluation of Wind Tunnel Tests on AFMDC Monorail Cone- and Spike-Nose Sled Configurations at Mach numbers from 2.0 to 5.0." AEDC-TR-68-198 (AD679206), December 1968.

2. Rhudy, R. W. and Corce, J. D. "Static Force and Moment Tests of the Holloman Narrow-Gage Rocket Sled at Mach Numbers from 1.5 to 4.0." AEDC-TR-75-29, August 1975.

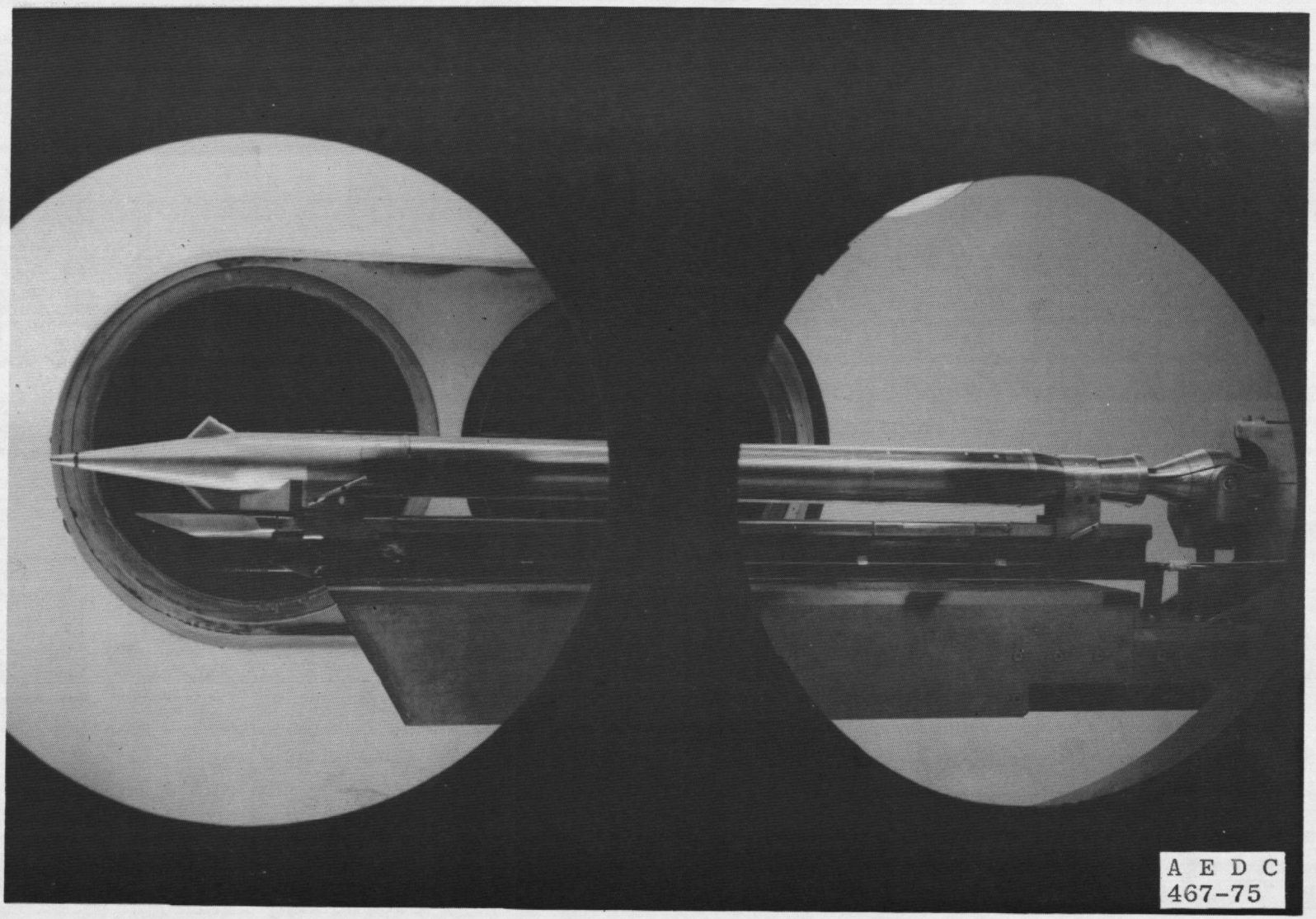

Figure 1. Monorail Sled Model installed in Tunnel B.

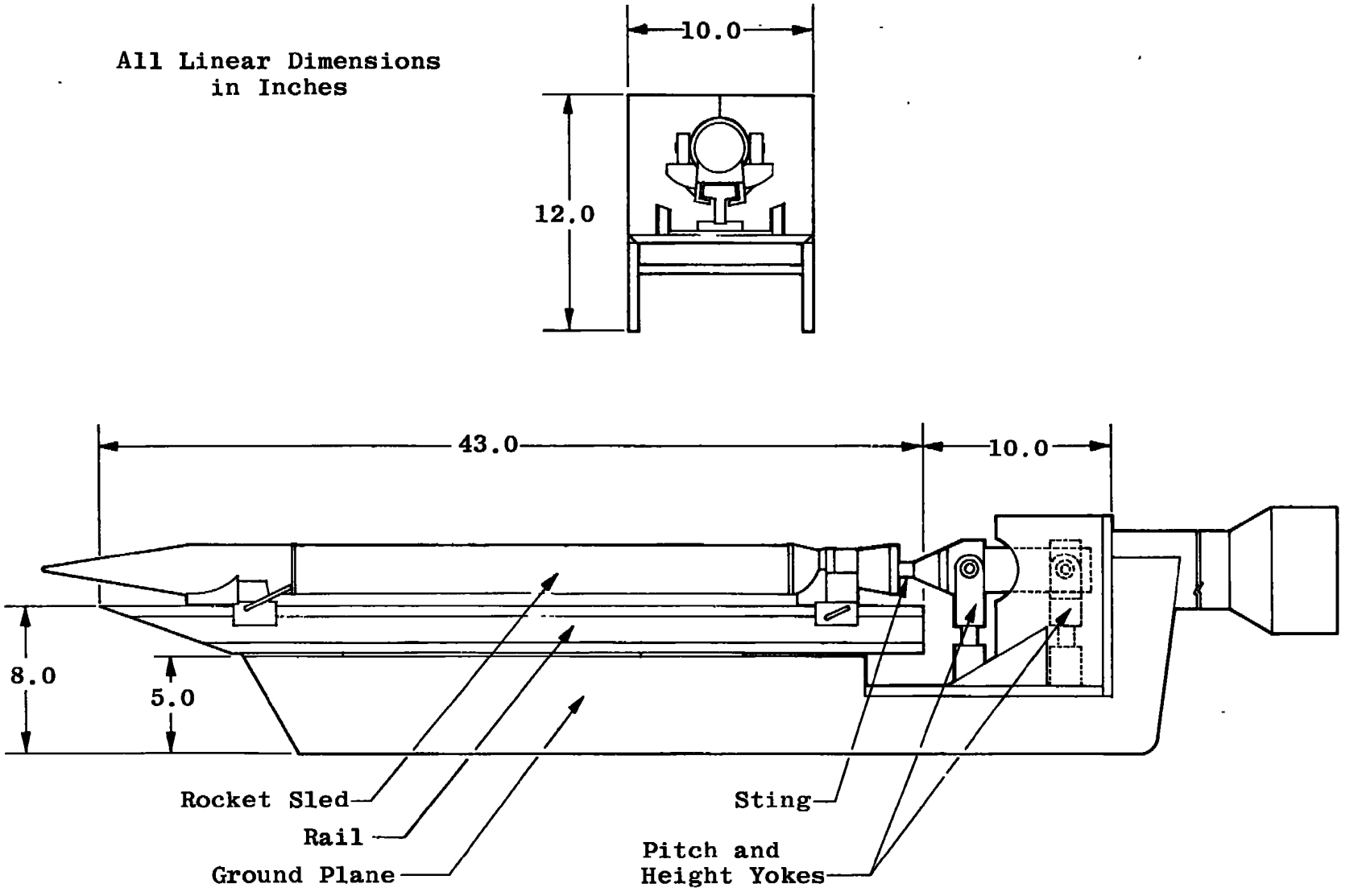

Figure 2. Model, sting, and ground plane assembly.

Nose	Dimension A	B	C	ℓ
1	25.59	45.22	1.90	31.56
	19.59	39.22	1.90	25.56
2,3	25.59	47.20	1.68	30.31
	19.59	41.20	1.68	24.31
4	25.59	45.80	1.90	30.71
	19.59	39.80	1.90	24.71

Moment Reference Point Is on Sled Body Centerline

All Linear Dimensions in Inches

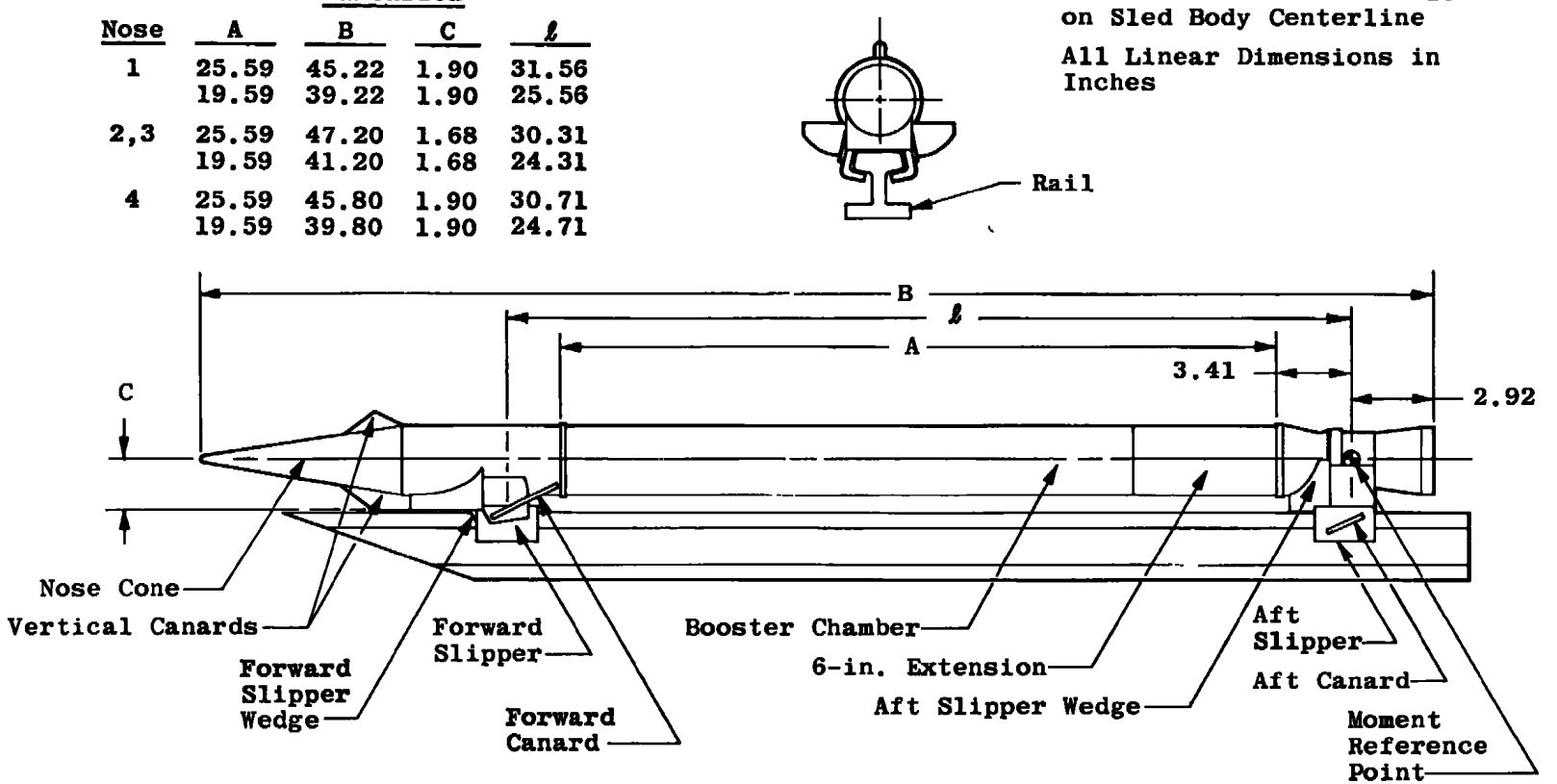

Figure 3. Model details.

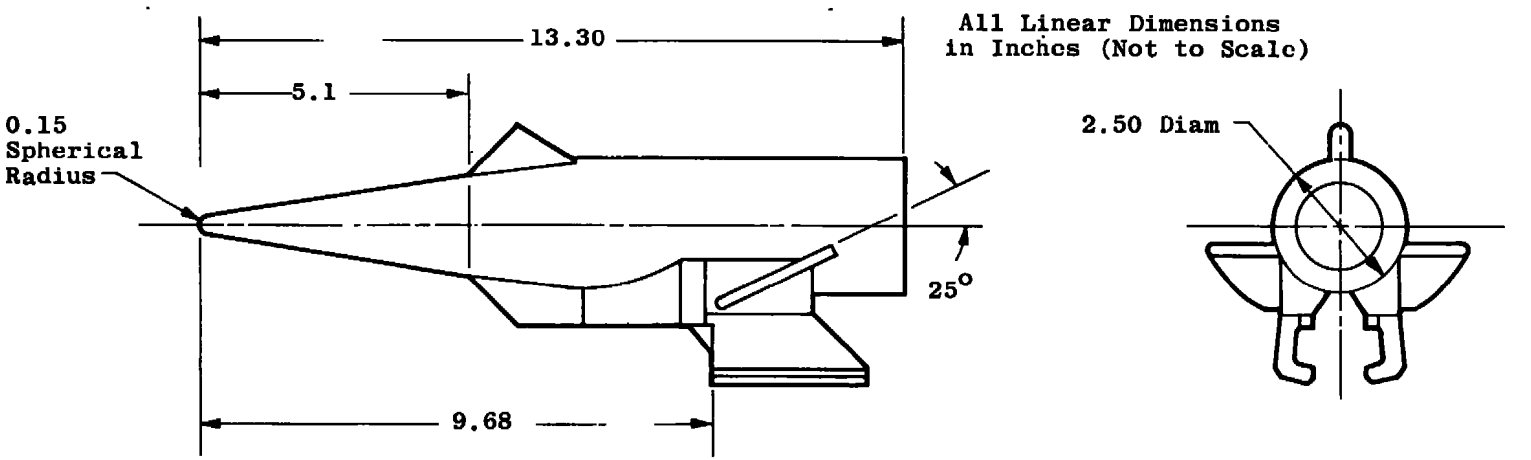

a. Nose 1, standard 18-deg (included angle) cone

Figure 4. Nose shape details.

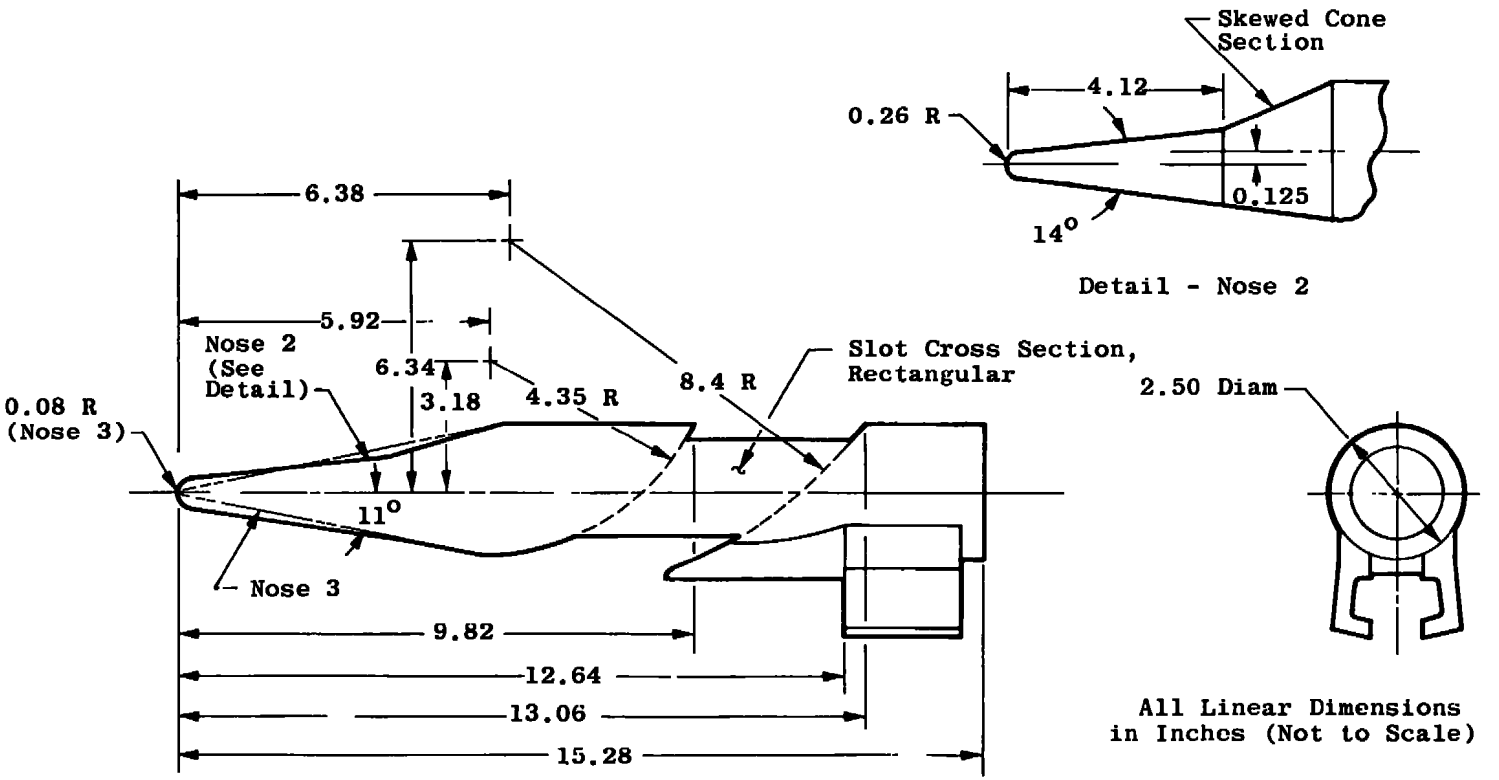

b. Nose 2, biconic 14-deg (included angle) shock ingestion; Nose 3, standard 22-deg (included angle) shock ingestion

Figure 4. Continued.

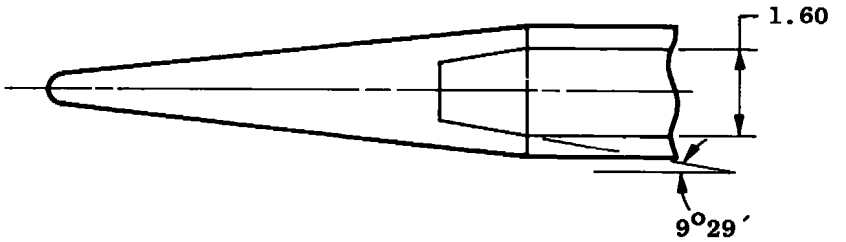

Section A-A
(Shown without Slipper)

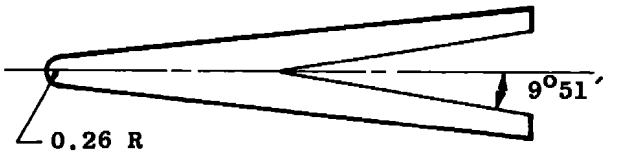

Section B-B
(Shown without Slipper)

All Linear Dimensions
in Inches (Not to Scale)

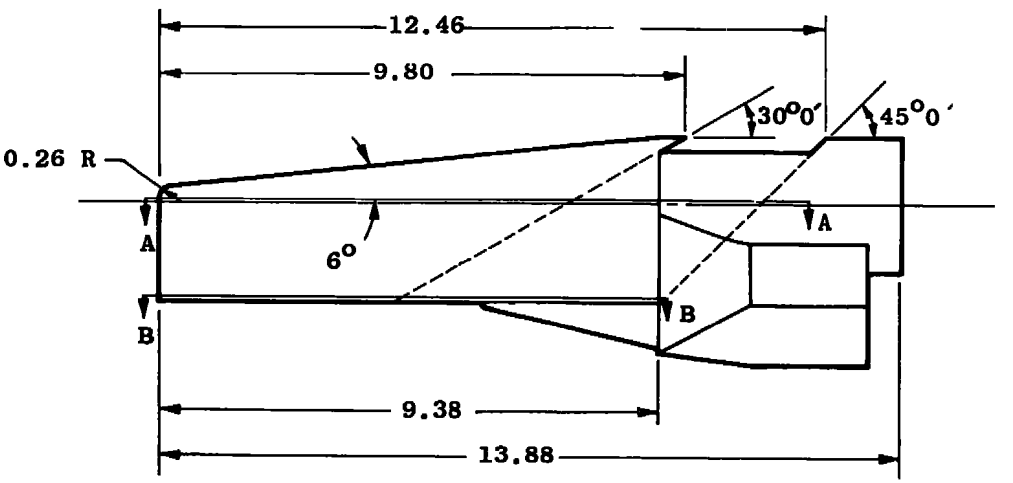

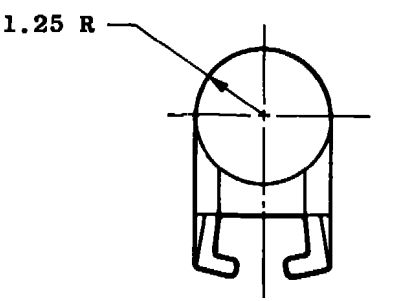

c. Nose 4, 6-deg (half cone) shock ingestion

Figure 4. Concluded.

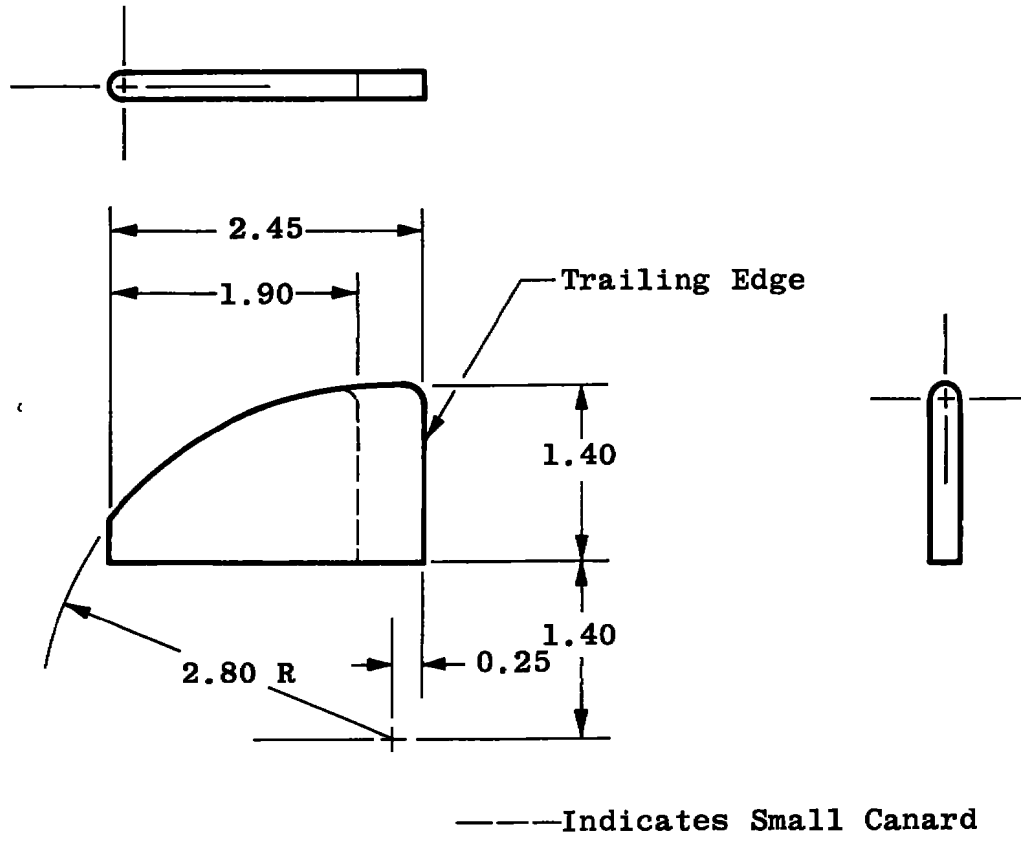

a. Forward canard

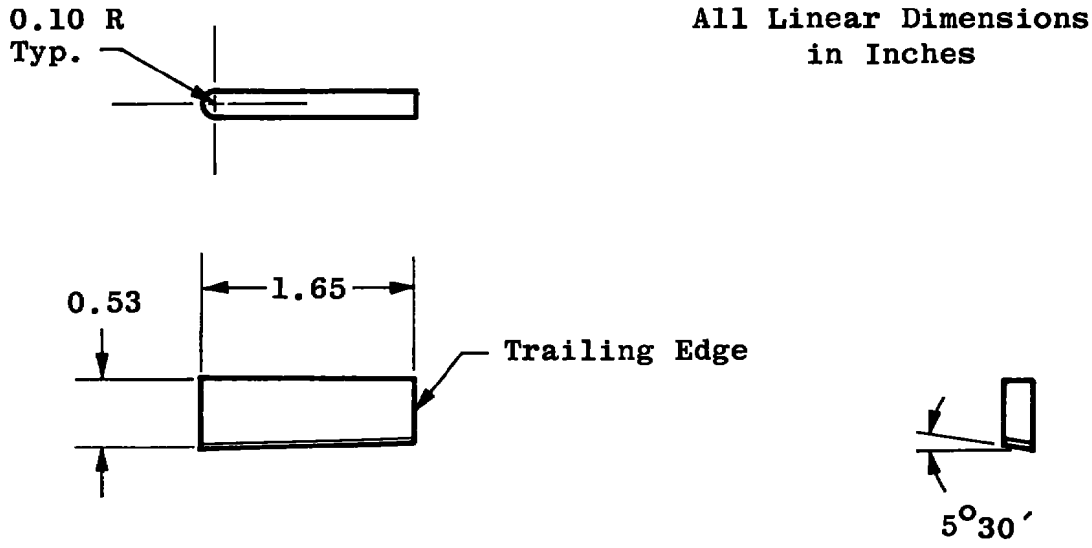

b. Aft canard

Figure 5. Forward and aft canard details.

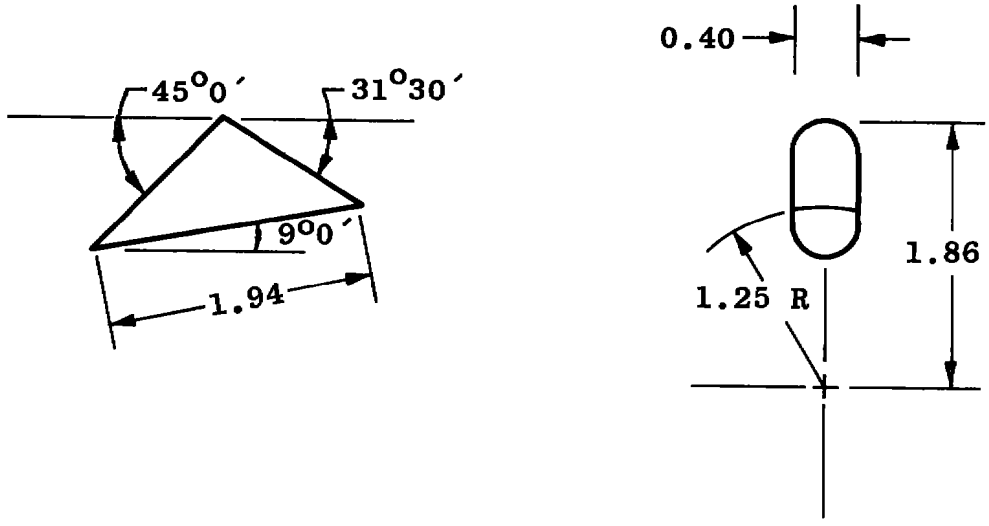

a. Upper vertical canard

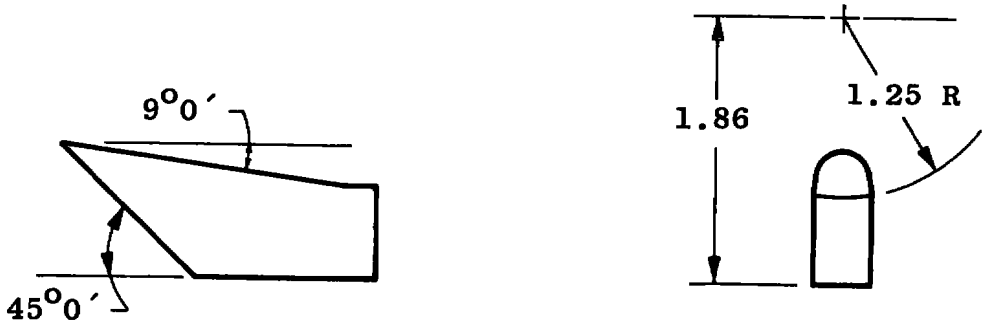

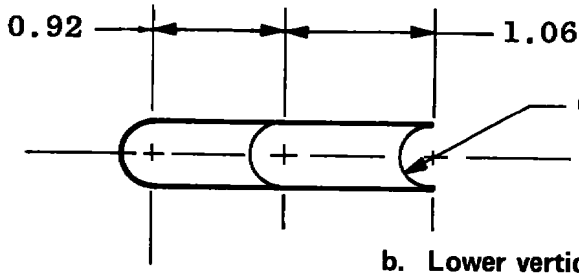

All Linear Dimensions in Inches

b. Lower vertical canard

Figure 6. Vertical canard details.

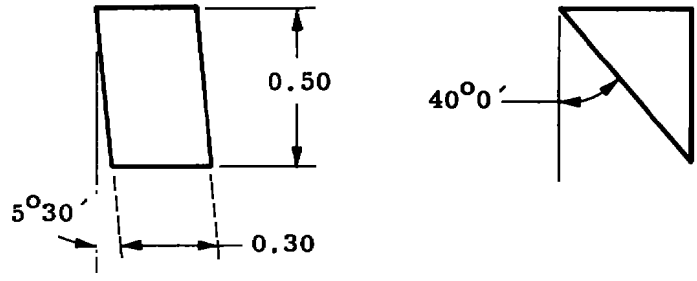

a. Forward slipper wedge

All Linear Dimensions
in Inches (Not to Scale)

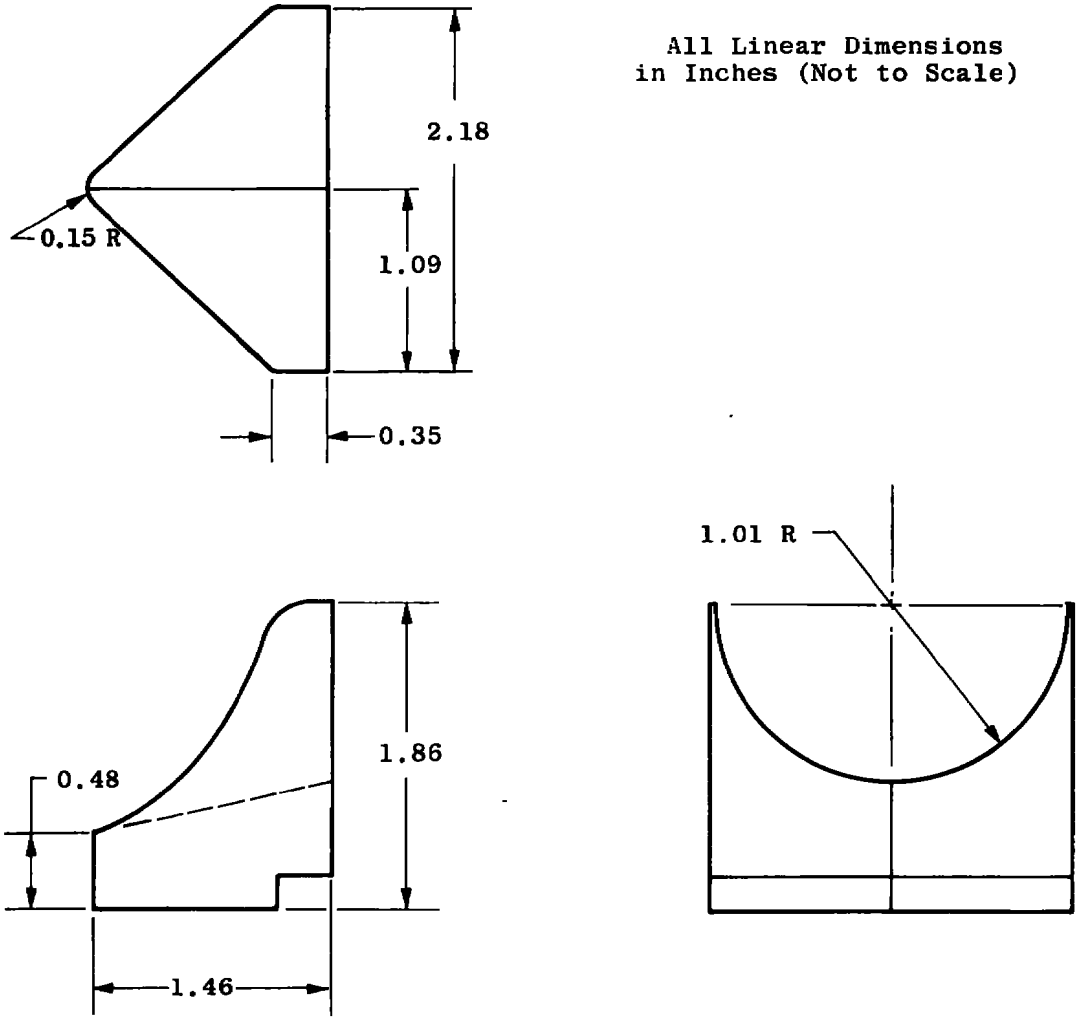

b. Aft slipper wedge

Figure 7. Forward and aft wedge details.

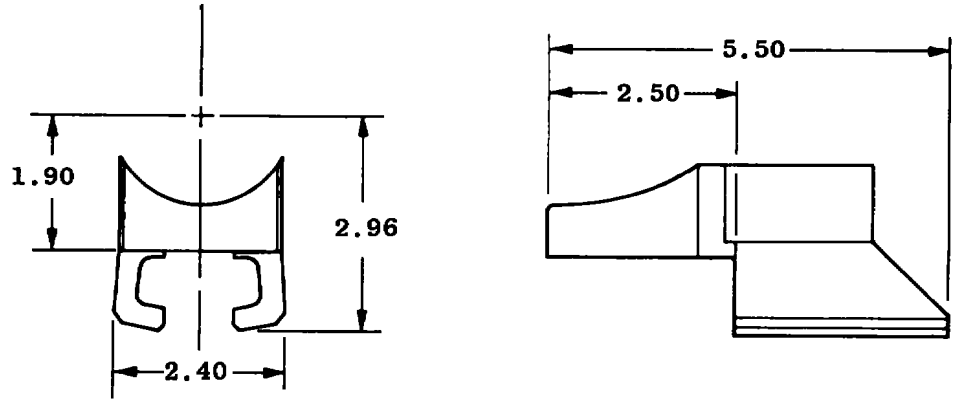

a. Forward slipper, nose 1

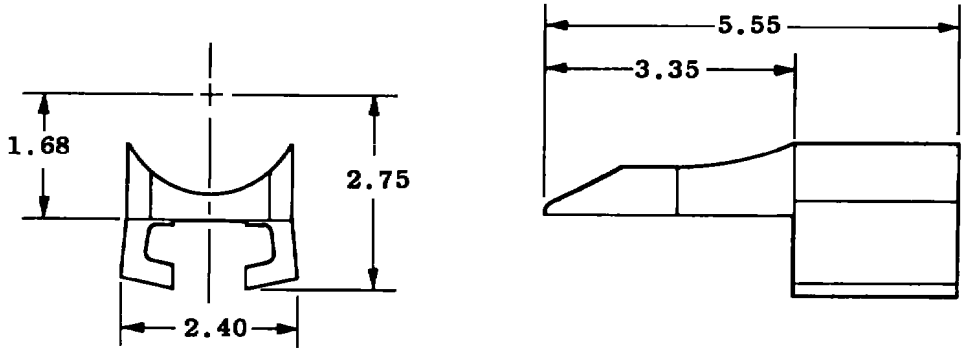

b. Forward slipper, noses 2 and 3

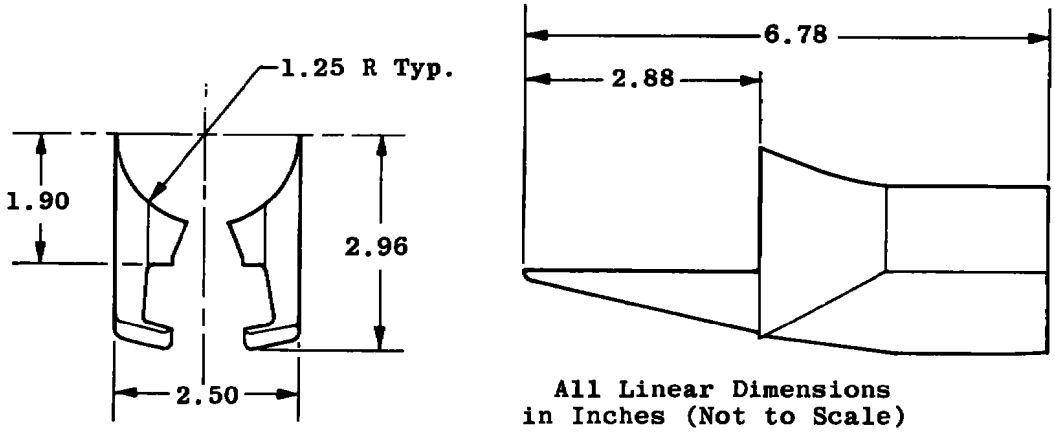

c. Forward slipper, nose 4

Figure 8. Forward and aft slipper details.

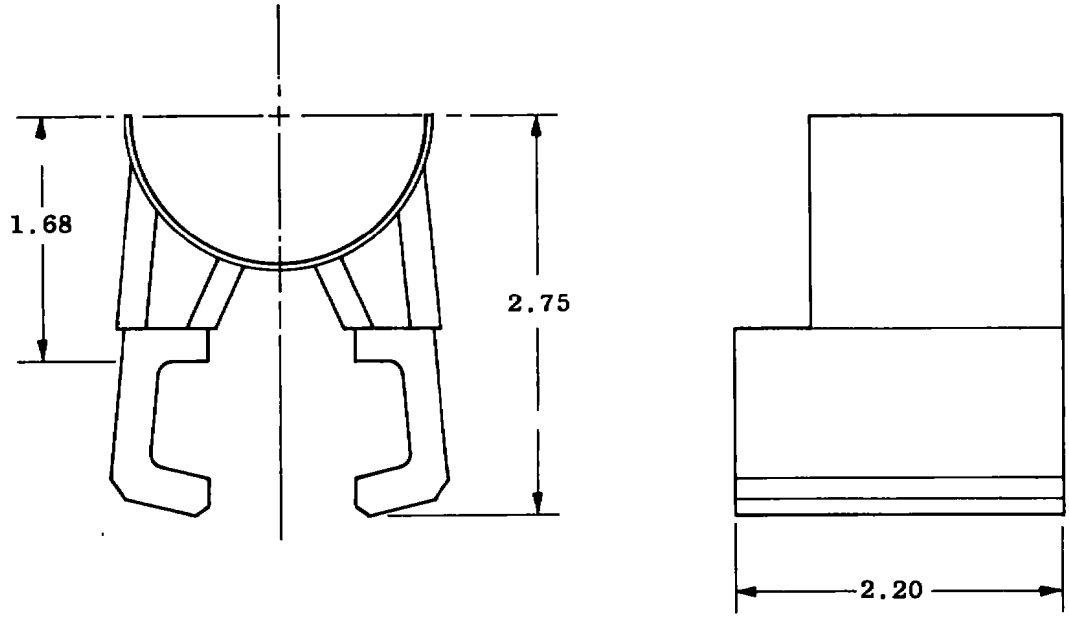

All Linear Dimensions
in Inches (Not to Scale)

d. Aft slipper, noses 2 and 3

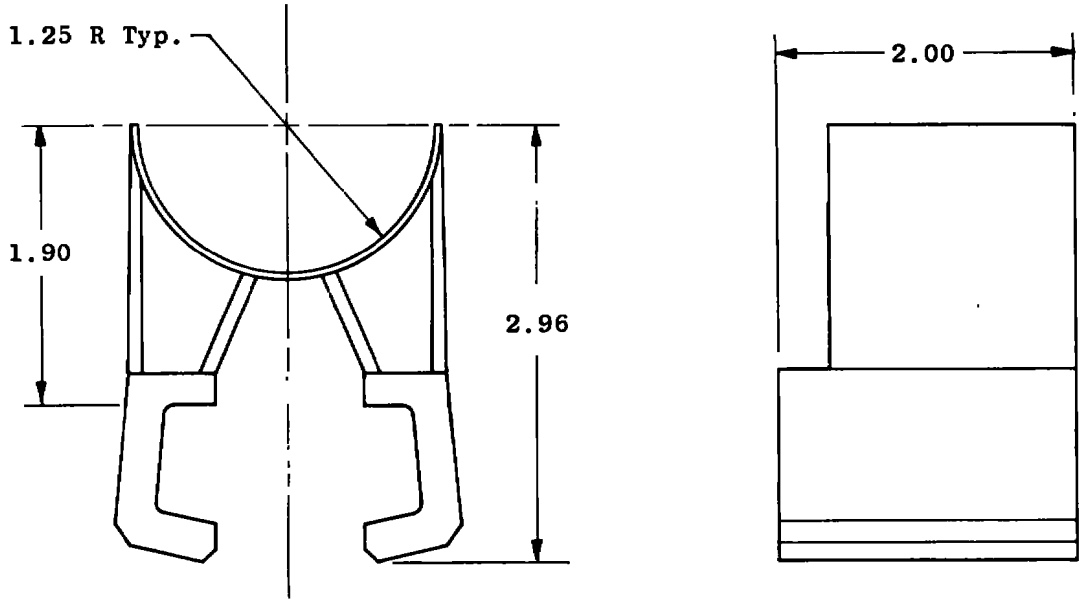

e. Aft slipper, noses 1 and 4

Figure 8. Concluded.

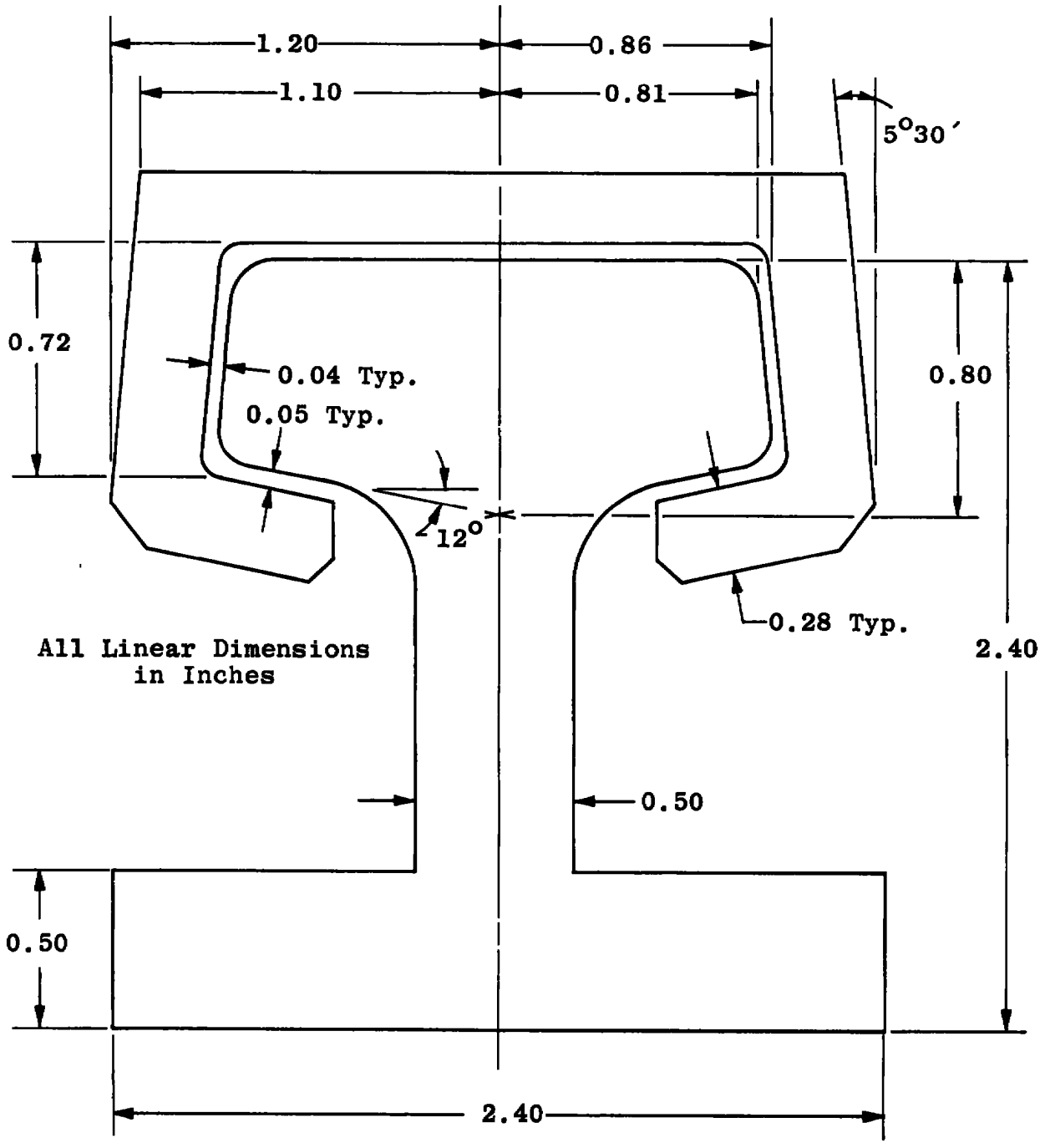

Figure 9. Typical slipper and rail cross section.

Nose 1
(Standard, 18-deg cone)

Nose 3
(22-deg shock ingestion)

Figure 10. Typical shadowgraph photographs, $M_\infty = 8$.

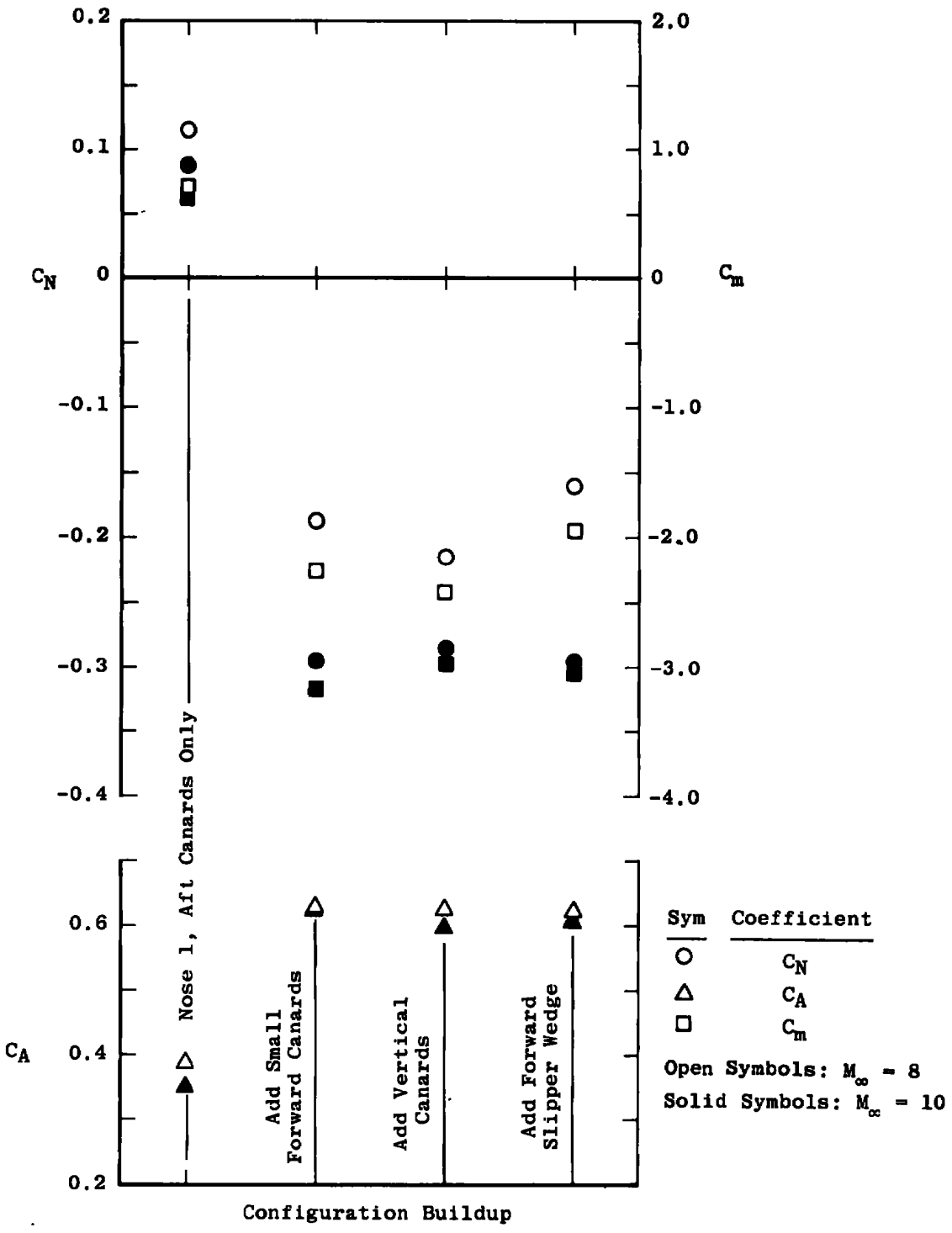

Figure 11. Configuration buildup for 18-deg standard cone.

Table 1. Tunnels B and C Data Summary for 0.4-percent Scale Model

Configuration							Sled Coefficients							
							$M_\infty = 8.0$				$M_\infty = 10.0$			
Nose Shape	Aft Slipper Wedge	Fwd Canards	Aft Canards	Vert Canards	Fwd Slipper Wedge	Booster Length, in.	C_N	C_m	C_{A_t}	C_A	C_N	C_m	C_{A_t}	C_A
1	Off	Off	Off	On	On	25.587	0.1577	1.1452	0.3118	0.3599	---	---	---	---
		Off	Off			19.587	---	---	---	---	0.1224	0.8327	0.3368	0.3550
		Small	On				-0.1607	-1.9439	0.6043	0.6209	-0.2965	-3.1521	0.5920	0.6014
					Off		-0.2155	-2.4175	0.6035	0.6251	-0.2861	-2.9908	0.5853	0.5941
				Off			-0.1879	-2.2652	0.6296	0.6276	-0.2955	-3.1976	0.6202	0.6225
	On						-0.1947	-2.3077	0.6283	0.6382	-0.2974	-3.1878	0.6174	0.6212
	Off		Off				-0.2032[a]	-2.2305[a]	0.6032[a]	0.6003[a]	-0.2733	-3.0921	0.5845	0.5861
		Off	On				0.1115	0.7147	0.3932	0.3895	0.0890	0.6730	0.3422	0.3448
		Large		On	On	25.587	-0.3778[a]	-4.1558[a]	0.6158[a]	0.6588[a]	---	---	---	---
				On	Off	19.587	-0.3718	-3.6297	0.6405	0.6354	---	---	---	---
				Off			-0.3007[a]	-3.0506[a]	0.6520[a]	0.6458[a]	---	---	---	---
	On						-0.2466	-2.7641	0.6666	0.6704	---	---	---	---
	Off		Off				-0.2823[a]	-2.9730[a]	0.6424[a]	0.6382[a]	---	---	---	---
2		Off	On			25.587	-0.2027[a]	-1.5940[a]	0.2519[a]	0.2974[a]	-0.1095	-1.5362	0.2262	0.2566
2						19.587	---	---	---	---	-0.0949	-1.2024	0.2352	0.2504
3						25.587	-0.2118[a]	-1.7796[a]	0.2751[a]	0.3296[a]	-0.0797	-1.6094	0.2767	0.3041
3						19.587	---	---	---	---	-0.0822	-1.2785	0.2728	0.2865
4						19.587	-0.0660	-0.8057	0.3134	0.3393	0.0049	-0.2476	0.2794	0.2900

[a]Contact between the slipper and rail may have occurred during data acquisition.

Note: $\alpha = 0$

Table 2. Calculated Full-Scale Loads for 4,000-ft Altitude (p_∞ = 12.7 psia)

Configuration							M_∞ = 8.0				M_∞ = 10.0			
Nose Shape	Aft Slipper Wedge	Fwd Canards	Aft Canards	Vert Canards	Fwd Slipper Wedge	Booster Length, ft	Fwd[a] Slipper, F_{N_F}, lb	Aft[b] Slipper, F_{N_A}, lb	Moment[c], ft-lb	F_A, lb	Fwd[a] Slipper, F_{N_F}, lb	Aft[b] Slipper, F_{N_A}, lb	Moment[c], ft-lb	F_A, lb
1	Off	Off	Off	On	On	5.33	2,420	1,780	15,900	9,600	---	---	---	---
		Off	Off			4.08	---	---	---	---	3,400	1,700	18,060	14,740
		Small	On				-5,070	790	-26,990	16,550	-12,850	500	-68,390	25,050
					Off		-6,310	560	-33,570	16,660	-12,200	280	-64,890	24,750
				Off			-5,910	900	-31,450	16,740	-13,040	729	-69,380	25,930
	On						-6,020	830	-32,040	17,020	-13,000	610	-69,160	25,880
	Off		Off				-5,820	400	-30,970	16,000	-12,610	1,230	-67,090	24,420
		Off	On				1,870	1,110	9,920	10,380	2,740	960	14,600	14,360
		Large		On	On	5.33	-8,800	-1,280	-57,700	17,560	---	---	---	---
				On	Off	4.08	-9,470	-440	-50,400	16,940	---	---	---	---
				Off			-7,960	-60	-42,360	17,220	---	---	---	---
	On						-7,210	640	-38,380	17,870	---	---	---	---
	Off		Off				-7,760	230	-41,280	17,010	---	---	---	---
2		Off	On			5.33	-3,340	-1,800	-21,020	7,530	-5,020	690	-31,640	10,150
2						4.08	---	---	---	---	-3,930	180	-24,770	9,900
3						5.33	-3,724	-1,640	-23,460	8,340	-5,263	2,110	-33,150	12,030
3						4.08	---	---	---	---	-4,180	940	-26,340	11,330
4						4.08	-2,350	450	-12,060	9,750	-1,126	1,360	-5,790	13,020

a. $F_{N_F} = C_m\,(d/\ell)\,S_{FS}\,q_{\infty_{FS}}$

b. $F_{N_A} = F_{N_T} - F_{N_F}$

c. Referenced at Centerline of Aft Slipper

Note: $\alpha = 0$

NOMENCLATURE

A_b	Cross-sectional area at the base, 4.909 in.^{2}
C_A	Forebody axial-force coefficient, $C_{A_t} - C_{A_b}$
C_{A_b}	Base axial-force coefficient, $- C_{p_b}(A_b/S)$
C_{A_t}	Total axial-force coefficient, total axial force/$q_\infty S$
C_m	Pitching-moment coefficient, (about ℄ of aft slipper, see Fig. 3), pitching moment/$q_\infty Sd$
C_N	Normal-force coefficient, normal force/$q_\infty S$
C_{p_b}	Base pressure coefficient, $(p_b - p_\infty)/q_\infty$
d	Diameter of sled model, 2.5 in.
F_A	Forebody axial force, lb
F_N	Normal force, lb
M_y	Pitching moment, ft-lb
M_∞	Free-stream Mach number
p_b	Average base pressure, psia
p_o	Free-stream stagnation pressure, psia
p_∞	Free-stream static pressure, psia
q_∞	Free-stream dynamic pressure, psia
$Re_{\infty,d}$	Free-stream Reynolds number based on sled diameter
S	Total projected frontal area of sled model (7.503 in.^{2}-N_1; 7.124 in.^{2}-N_2 and N_3; 8.090 in.^{2}-N_4)
T_o	Free-stream stagnation temperature, °R

SUBSCRIPTS

A	Aft
F	Forward
FS	Full scale
T	Total